Acta Biomaterialia 138 (2022) 301–312

Contents lists available at ScienceDirect

Acta Biomaterialia

journal homepage: www.elsevier.com/locate/actbio

Full length article

# Structural aspects controlling the mechanical and biological properties of tough, double network hydrogels

Yuwan Huang[a], Pavithra B. Jayathilaka[b], Md Shariful Islam[c], Carina B. Tanaka[a], Meredith N. Silberstein[d], Kristopher A. Kilian[b,c], Jamie J. Kruzic[a,*]

[a] School of Mechanical and Manufacturing Engineering, University of New South Wales (UNSW Sydney), Sydney NSW 2052, Australia
[b] School of Chemistry, Australian Centre for NanoMedicine, University of New South Wales (UNSW Sydney), Sydney NSW 2052, Australia
[c] School of Materials Science and Engineering, University of New South Wales (UNSW Sydney), Sydney NSW 2052, Australia
[d] Sibley School of Mechanical and Aerospace Engineering, Cornell University, Ithaca, NY, USA

ARTICLE INFO

*Article history:*
Received 22 August 2021
Revised 12 October 2021
Accepted 25 October 2021
Available online 29 October 2021

*Keywords:*
Polyethylene glycol
Alginate
Double network hydrogels
Mechanical properties
Compressive strength
Toughness

ABSTRACT

Anticipating an increasing demand for hybrid double network (DN) hydrogels in biomedicine and biotechnology, this study evaluated the effects of each network on the mechanical and biological properties. Polyethylene glycol (PEG) (meth)acrylate hydrogels with varied monomer molecular weights and architectures (linear vs. 4-arm) were produced with and without an added ionically bonded alginate network and their mechanical properties were characterized using compression testing. The results showed that while some mechanical properties of PEG single network (SN) hydrogels decreased or changed negligibly with increasing molecular weight, the compressive modulus, strength, strain to failure, and toughness of DN hydrogels all significantly increased with increased PEG monomer molecular weight. At a fixed molecular weight (10 kDa), 4-arm PEG SN hydrogels exhibited better overall mechanical performance; however, this benefit was diminished for the corresponding DN hydrogels with comparable strength and toughness and lower strain to failure for the 4-arm case. Regardless of the PEG monomer structure, the alginate network made a relatively larger contribution to the overall DN mechanical properties when the covalent PEG network was looser with a larger mesh size (e.g., for larger monomer molecular weight and/or linear architecture) which presumably enabled more ionic crosslinking. Considering the biological performance, adipose derived stem cell cultures demonstrated monotonically increasing cell area and Yes-associated protein related mechanosensing with increasing amounts of alginate from 0 to 2 wt.%, demonstrating the possibility for using DN hydrogels in guiding musculoskeletal differentiation. These findings will be useful to design suitable hydrogels with controllable mechanical and biological properties for mechanically demanding applications.

**Statement of significance**

Hydrogels are widely used in commercial applications, and recently developed hybrid double network hydrogels have enhanced strength and toughness that will enable further expansion into more mechanically demanding applications (e.g., medical implants, etc.). The significance of this work is that it uncovers some key principles regarding monomer molecular weight, architecture, and concentration for developing strong and tough hybrid double network hydrogels that would not be predicted from their single network counterparts or a linear combination of the two networks. Additionally, novel insight is given into the biological performance of hybrid double network hydrogels in the presence of adipose derived stem cell cultures which suggests new scope for using double network hydrogels in guiding musculoskeletal differentiation.



## 1. Introduction

Hydrogels are widely used in commercial applications such as contact lenses [1,2], wound dressings [3,4], drug delivery [5], tissue engineering scaffolds [6,7], etc. However, further expansion of hy-

* Corresponding author.
*E-mail address:* j.kruzic@unsw.edu.au (J.J. Kruzic).

https://doi.org/10.1016/j.actbio.2021.10.044
1742-7061/

drogel usage into applications that require mechanical strength and toughness (e.g., medical implants, soft robotics, etc.) is limited by the weakness and brittleness of conventional single network (SN) hydrogels. To address these limitations, there has been considerable research interest in the development of strong and tough hydrogels including double network (DN) hydrogels [8–15], slide-ring hydrogels [16,17], tetra-PEG hydrogels [18], dual-crosslinked hydrogels [19,20], supramolecular hydrogels [21,22], hydrogels toughened by longer and stronger polymer chains [23–25], etc. These advanced hydrogel systems possess high strength and toughness and allow for other advantages such as stimuli-responsiveness [26]. DN hydrogels were first introduced by Gong et al. using poly(2-acrylamido-2-methylpropanesulfonic acid) (PAMPS) and polyacrylamide (PAAm) [8]. Compared to conventional SN gels where the toughness is only ~0.1–1 J/m$^2$, PAMPS/PAAm DN gels showed much higher toughness of 100–1000 J/m$^2$ along with high stiffness (0.1–10 MPa), high tensile strength (1–10 MPa) and high compressive strength (20–60 MPa) [8,27]. Inspired by this success, many other advanced hydrogel systems consisting of two different covalent networks have been developed with excellent mechanical performance [9–14]. However, one limitation of covalently bonded DN hydrogels is that the energy dissipating bond breakage mechanism that gives high toughness also causes permanent damage to the network that cannot be recovered, for example in cases of repeated or cyclic loading.

Further research to address this issue brought about the development of highly stretchable and tough hybrid DN hydrogels with self-healing properties by introducing a physically bonded network to reinforce a covalently bonded hydrogel [28]. In the initial study using sodium alginate to reinforce PAAm, impressive properties including stretch of ~21× and toughness of ~9000 J/m$^2$ were demonstrated for the hybrid DN gels [28]. Among possible physically bonded networks, sodium alginate networks formed using cation crosslinkers (e.g., $Ca^{2+}$) present an attractive option with low toxicity, relatively low cost, quick and easy polymerization, excellent biocompatibility, and adaptability for mechanochemistry [13,26,28–32]. As an example, alginate/poly(ethylene glycol) diacrylate (PEGDA) hybrid DNs showed excellent mechanical properties as well as great flexibility to encapsulate human mesenchymal stem cells and also allowed for 3D printing into complex scaffold structures [13].

Polyethylene glycol (PEG) and its various derivatives are considered attractive for biomedical hydrogel applications because of their hydrophilic nature, stable covalent bonding structure, biocompatibility, and their potential for bioactive modification with various functional end groups [33–42]. For SN PEG-based hydrogels, research has been conducted to determine how the mechanical properties (e.g., stiffness) and biological properties (e.g., protein diffusion, accumulation, and release) can be controlled by varying the molecular weight, concentration, and/or architecture (linear, 4-arm, or 8-arm) of the PEG monomers as well as the crosslinking mechanism [35,36,39–43]. Furthermore, mechanical and biological properties are not thought to be independent and varying the stiffness of PEG-based and other SN hydrogels is well known to influence the differentiation and proliferation behavior of cells [40,44–47].

When considering how to control the mechanical and biological properties of hybrid DN hydrogels, there are many variables to consider and relatively little is known. The first study on alginate/PAAm hybrid gels found a higher ratio of alginate to PAAm leads to higher stiffness and tensile strength while the stretch and fracture energy peaked at around 11–14 wt.% alginate [28]. While increasing the amount of covalent N,N′-methylenebisacrylamide (MBAA) or ionic $Ca^{2+}$ crosslinkers has generally been found to stiffen hybrid DN hydrogels, the effects on strength and toughness are more complex and have shown some variability across studies [28,48]. Finally, while studies of alginate/PEGDA hybrid gels have suggested the single networks with higher toughness lead to tougher double networks [13], little has been reported about other properties or more detailed structure-property relationships. Overall, to further enable the design and development of strong and tough hybrid DN hydrogels there is a need to understand how network characteristics such as monomer molecular weight and architecture (e.g., linear vs. 4-arm) influence the overall mechanical properties. Furthermore, while there have been a few studies demonstrating promising results regarding how hybrid double networks of gellan gum/PEGDA or glycol chitosan/alginate can favorably promote spreading and proliferation of mesenchymal stem cells [49,50], further details regarding how to control the biological performance of DN hydrogels are still poorly understood.

Accordingly, the goal of this work is to uncover some key principles for developing strong and tough hybrid DN hydrogels suitable for biomedical applications. The primary focus of this work is on how molecular weight (MW) and architecture (linear vs. 4-arm) of the covalently linked monomers affect the mechanical behavior of DN gels reinforced with a physically bonded network. We have selected PEG (meth)acrylate for the covalent networks and sodium alginate for the physically bonded networks due to their attractive mechanical and biocompatibility properties. Secondly, this works seeks to increase our understanding of how cells sense and respond to the altered mechanical properties of hybrid double network gels.

## 2. Materials and methods

### 2.1. Materials

Linear poly(ethylene glycol) diacrylate (PEGDA, MW 2 kDa and 5 kDa, see Fig. 1a) and 4-arm poly(ethylene glycol) acrylate (PEG4AC, MW 10 kDa and 20 kDa, see Fig. 1c) were supplied by JenKem Technology USA Inc.. Linear poly(ethylene glycol) dimethacrylate (PEGDMA, MW 10 kDa, see Fig. 1b) was synthesized using dried PEG supplied by Sigma-Aldrich as described previously [37,51]. Briefly, 10 kDa PEG (Sigma-Aldrich) dissolved in toluene was dehydrated twice in an evaporator and then dissolved in a mixture of toluene, dichloromethane, and triethylamine to react with 2.2× equivalence of methacrylic anhydride for 2 days at room temperature. After mixing with potassium carbonate, the as-synthesized PEGDMA was filtered and precipitated with added diethyl ether. The PEGDMA after final vacuum filtration was stored at -20°C for subsequent use. The photoinitiator 2-hydroxy-4′-(2-hydroxyethoxy)-2-methylpropiophenone (I2959) was purchased from Sigma-Aldrich Australia. Calcium chloride and sodium alginate were purchased from ChemSupply Australia.

### 2.2. Fabrication of hydrogels

Desired hydrogel compositions (e.g., gel fractions) were achieved by controlling the weight fractions of PEG and alginate powder in the pregel solution. Linear and 4-arm PEG (meth)acrylate SN hydrogels, as schematically shown in Fig. 1d, were prepared by dissolving PEG (meth)acrylate powder in deionized water to a concentration of 10 wt.%. One additional linear 5 kDa PEGDA group was produced at a concentration of 5 wt.%. The photoinitiator, I2959, was dissolved in 80% (v/v) ethanol to keep a solid-liquid ratio of 0.1 mmol per 1 mL. Then the I2959 solution was added into the pregel mixture at a concentration of 50 µL photoinitiator solution to 0.01 mmol PEG monomers. The precursor solution was then poured into glass molds which consisted of two cover slips and one silicone spacer of ~5 mm in height. The gel sheets were polymerized using ultraviolet (UV) irradiation in a UV source instrument (either Spectronics XL-1000 UV crosslinker

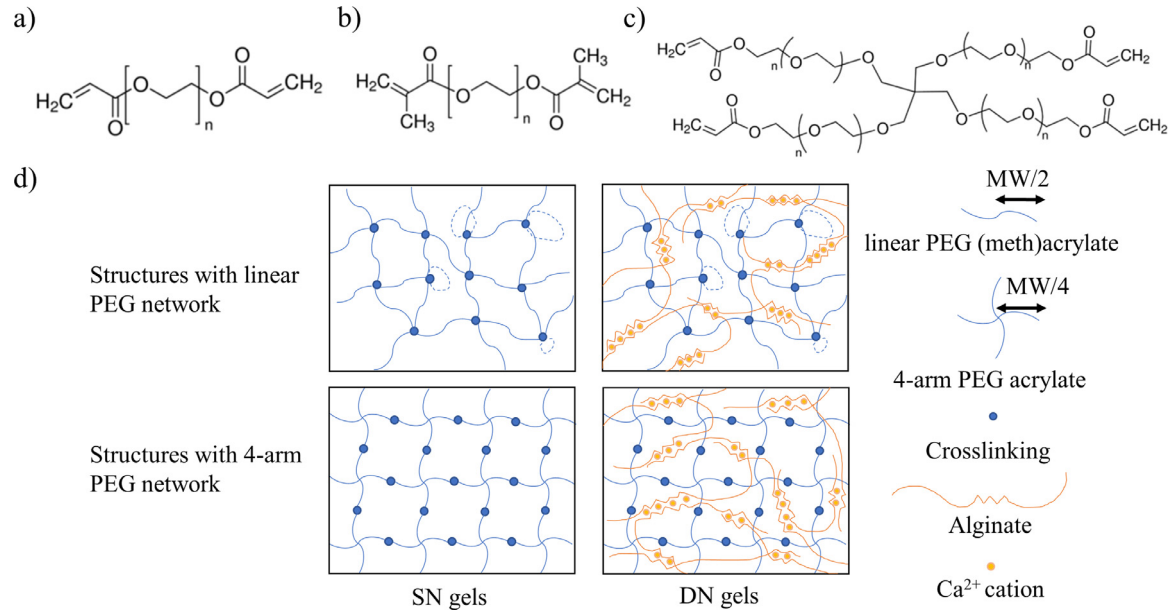


**Fig. 1.** (a) Chemical structure of PEGDA. (b) Chemical structure of PEGDMA. (c) Chemical structure of PEG4AC. (d) Network structures of PEG-based SN and DN hydrogels. Linear (top) and 4-arm (bottom) monomers are expected to form different covalent PEG networks at a given molecular weight (MW). To get a similar mesh size for the 4-arm PEG network, approximately half the molecular weight would be required compared to the linear PEG network.

**Table 1**
Single (SN) and hybrid double network (DN) hydrogels used in this work.

| | Covalent PEG network | | | Tested groups | | |
|---|---|---|---|---|---|---|
| | Monomers | MW | Mass fraction | SN gels | DN gels | |
| Linear groups | PEGDA | 2 kDa | 10 wt.% | + 0 wt.% alginate | + 1 wt.% alginate | + 2 wt.% alginate |
| | PEGDA | 5 kDa | 5 wt.% | | | |
| | PEGDA | 5 kDa | 10 wt.% | | | |
| | PEGDMA | 10 kDa | 10 wt.% | | | |
| 4-arm groups | PEG4AC | 10 kDa | 10 wt.% | | | |
| | PEG4AC | 10 kDa | 10 wt.% | | | |

or Rayonet RMR-600 photochemical reactor). Photopolymerization time varied from 30 min to 2 h to ensure adequate gelation with increasing times used for decreasing molecular weight. Cylindrical samples for subsequent mechanical testing were cut from the cured gel sheets using a sharpened brass tube cutter with an inner diameter of ~4.8 mm and then were kept in a sealed and moist container.

For the DN hydrogels, concentrations of 1 and 2 wt.% alginate were added to the above-described SN pregel mixtures prior to photoinitiation. First, the covalent network was cured in the glass mold in the presence of UV crosslinker for the same time as for the SN gels, and then the gel was soaked in 0.1 M $CaCl_2$ solution for more than 2 hours to crosslink the ionically bonded alginate network. Then, cylindrical samples were cut from the cured gel sheets as described above and were kept in a sealed and moist container. A summary of all SN and DN hydrogel groups is given in Table 1.

### 2.3. Gel swelling measurement

The initial weight, $W_0$, diameter, $D_0$, and height, $h_0$, of the as-prepared gels were measured after cutting. The samples were then kept in a 24-well tissue culture plate with 0.4 mL 0.1 M $CaCl_2$ solution overnight in a refrigerator. Then, the dimensions ($D_w$ and $h_w$) and weight ($W_w$) of the swollen gels were measured again before testing. The swelling ratio was calculated as the ratio of increased weight to initial weight, $\frac{W_w - W_0}{W_0}$, while the swelling stretch was calculated based on the change in height, $\frac{h_w}{h_0}$.

### 2.4. Characterization of hydrogels

All compression tests were performed using an Instron 3369 universal testing machine with a calibrated 250 N load cell and a linear variable displacement transducer. At least five swollen cylindrical gel samples were tested for each group. During testing, samples were placed in a 34 mm diameter petri dish with 1.4 mL of 0.1 M $CaCl_2$ solution to prevent the samples from drying out. The cylindrical gel samples were compressed until failure using a displacement rate of 0.01 mm/sec. The 10 kDa PEG4AC group was used for additional comparison testing at higher strain rate of 0.1 mm/sec. Cyclic loading testing was also performed for the 10 kDa PEG4AC group whereby the samples were compressed to around 60% of the initial height at a displacement rate of 0.01 mm/sec and then released immediately at the same rate.

The engineering strain under compression was calculated as $\varepsilon_e = \frac{\Delta h}{h_w}$, where $\Delta h$ represents the difference between deformed height, $h_c$, and original height in the swollen state, $h_w$. The engineering stress was calculated as $\sigma_e = \frac{F}{A_w}$, where $F$ was the applied force and $A_w$ was the cross-sectional area of the undeformed wet, swollen gel sample. The compressive modulus was defined as the ratio of applied stress to strain on the sample in the initial region of the stress-strain curve and was determined by calculating the slope of a linear fitted trendline within the 5%-10% strain region. True strain and stress were calculated using the two equations $\varepsilon_t = ln\ \frac{h_c}{h_w} = -ln(1-\varepsilon_e)$ and $\sigma_t = \frac{F}{A_c} = \sigma_e(1-\varepsilon_e)$, where $h_c$

and $A_c$ are the height and cross-sectional area of the compressed gels, respectively. The toughness of the gels in compression was determined as the area under the true stress-strain curve up to the point of fracture for each sample. Similarly, energy dissipation during the cyclic loading tests was calculated as the difference in the area under the loading and unloading curves.

### 2.5. Mechanical modeling

Stress-strain data was fit to the incompressible Arruda-Boyce model using least-squares minimization via a custom MATLAB script. The statistical mechanics-derived form of this model for uniaxial tension/compression is given by $\sigma_t = \frac{1}{3} n k_b T \frac{N}{\lambda_{ch}} \mathcal{L}^{-1}\{\frac{\lambda_{ch}}{\sqrt{N}}\}(\lambda^2 - \frac{1}{\lambda})$, where $k_b$ is Boltzmann's constant, $T$ is the temperature in Kelvin, $\mathcal{L}$ is the Langevin function, $\lambda = 1 - \varepsilon_e$ is the stretch, and $\lambda_{ch} = \frac{1}{\sqrt{3}}\sqrt{\lambda^2 + \frac{2}{\lambda}}$ is the effective chain stretch [52]. The material constants here are "$n$" which describes the network crosslink density and "$N$" which describes the number of Kuhn segments between crosslinks. The model parameters, along with their swelling adjusted values, were used to quantitatively compare the effective polymer structures and provide insight into interpreting the mechanical testing results. The swelling adjustment was calculated based on the swelling stretch in terms of height and diameter measured for each sample. When the swelling stretch is positive the "as-fabricated" materials will have higher "$n$" and "$N$" values compared to the swollen state. These swelling adjusted parameters are particularly useful in understanding the failure strain since greater swelling means that the polymer chains will be in a more extended configuration before any mechanical stress is applied.

### 2.6. Cell culture and immunofluorescence analysis

For cell culture experiments, SN and DN hydrogel sheets produced from 10 wt.% 10 kDa PEGDMA with 0–2 wt.% alginate were prepared with ~1 mm thickness following the previous protocol. It is noted that PEG-based materials have sometimes been utilized for their antifouling properties, which is desirable for many biomedical applications to prevent unwanted physisorption. In our experiments, to promote cell adhesion we chemically conjugated fibronectin into the alginate network using carbodiimide chemistry as has been described in the literature [53,54]. Briefly, the method for sample preparation and fibronectin conjugation is as follows.

Gel sheets were cut into rectangular samples (approximately 10 mm × 10 mm × 1 mm) and were transferred into glass vials and rinsed twice with 2-(N-morpholino)-ethanesulfonic acid (MES) buffer (at pH=5.5) and incubated with gentle shaking for 5 minutes. Carboxylic acid groups of the alginate component were activated by the addition of water soluble carbodiimide 1-ethyl-(dimethylaminopropyl) carbodiimide (EDC) (0.1 M) followed by N-hydroxysulfosuccinimide sodium salt (sulfo-NHS; 0.1 M) and shaking for 20 minutes. Next, fibronectin (50 mg/ml) was added into the glass vial with gentle shaking for 1 h. The gels were washed twice with phosphate buffered saline (PBS) and transferred into a 12 well plate for cell seeding. Samples were then washed again using sterile PBS and sterilized by UV exposure for 30 minutes.

The adipose-derived mesenchymal stem cells (ADSCs, ATCC PCS-500-011) were cultured in low-glucose Dulbecco's modified Eagle's medium (Thermo Fisher Scientific, Cat. No. 11885084) supplemented with 1% (v/v) penicillin and streptomycin (Sigma Aldrich, Cat. No. P4333) and 10% (v/v) fetal bovine serum (BOVOGEN, Australia, Cat. No. SFBS-AU) at 37°C with 5% $CO_2$ in a humidified incubator. The medium was changed every 48 h and cells were passaged at 80–85% confluency. All ADSCs used in the experiments were at the passage number 5.

ADSCs were fixed with 4% paraformaldehyde (Sigma-Aldrich Pty Ltd.) for 30 min and permeabilized in 0.1% Triton X-100 (Sigma-Aldrich Pty Ltd.) in phosphate buffered saline (PBS) for 1 h. 1% bovine serum albumin (BSA) was employed to block the cells for 1 h. Yes-associated protein (YAP, 1:200) labelling was performed in 1% BSA (w/v) in PBS for 24 h at room temperature, followed by rinsing twice with PBS. Secondary antibody labelling was performed at 1:500 dilution in 1% BSA in PBS for 2 h at room temperature in the dark. Actin and nuclei were stained with 488-phalloidin (1:200) and Hoechst 33342 (1:1000), respectively. Immunofluorescence microscopy was conducted using a Zeiss LSM 800 confocal microscope. Cell area was measured from phalloidin staining of the actin cytoskeleton by measuring the average cell area of 30 cells per sample using ImageJ software. Cell nuclear YAP localization percentages were calculated by manually counting cells with nuclear co-localized YAP and finally dividing by the total number of cells and multiplying by 100.

### 2.7. Statistical analyses

Mechanical and biological data are reported as mean ± standard deviation (SD) and mechanical testing samples with obvious void defects noticed after fracture were removed from the analysis. For statistical analysis of swelling and mechanical properties, Levene's test revealed non-equal variances among many groups. Thus, a Kruskal-Wallis test was used to determine if each main independent variable had a significant effect and Dunn's post-hoc test was used for pairwise comparisons. These statistical tests were performed using SPSS software and a p-value smaller than 0.05 was considered statistically significant. For statistical analysis of the cell culture experiments, data was collected from 30 cells with three replicates for each hydrogel group that we tested. A one-way analysis of variance (ANOVA) with Tukey's HSD post-hoc analysis was performed using Origin software and again a p-value smaller than 0.05 was considered statistically significant.

## 3. Results

### 3.1. Swelling properties

To avoid degradation of the alginate network due to release of $Ca^{2+}$ cations, as synthesized hydrogels were stored in 0.1 M $CaCl_2$ solution to ensure saturation of the ionic crosslinking. Overall, the varied PEG monomer molecular weights and/or architectures did not result in any morphological differences in appearance of the hydrogels as viewed by optical microscopy. The change in weight and size after soaking overnight (>13 h) in $CaCl_2$ solution are presented in Fig. 2 for all 24 comparison groups. Both SN and DN gels demonstrated free and homogeneous swelling with similar swelling stretch in both diameter and height (diameter data not shown). Overall, hydrogels formed by larger MW monomers had significantly ($p < 0.05$) more swelling regardless of alginate reinforcement. For the double networks, adding alginate significantly ($p < 0.05$) reduced the swelling of the DN gels relative to the SN gels. Finally, when compared at the same MW of 10 kDa, the 4-arm PEG-based hydrogels swelled significantly ($p < 0.05$) less than their linear counterparts regardless of alginate reinforcement.

### 3.2. Mechanical characterization from quasistatic compression testing

Fig. 3a shows a representative compression true stress-strain curve for each SN gel. It is seen that SN gels formed by 4-arm monomers failed at approximately four times higher true stress than those produced from linear monomers at the same weight fraction. Fig. 3b shows example compression true stress-strain curves that illustrate the strengthening and toughening effect of

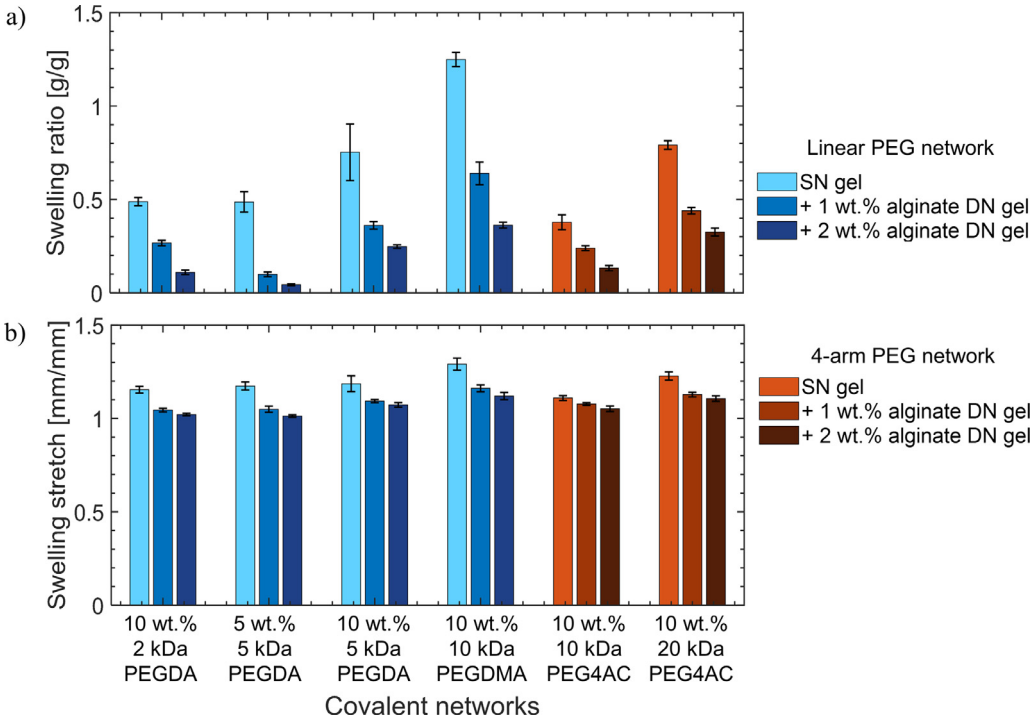


**Fig. 2.** (a) Swelling ratio and (b) swelling stretch of PEG-based SN and DN hydrogels.

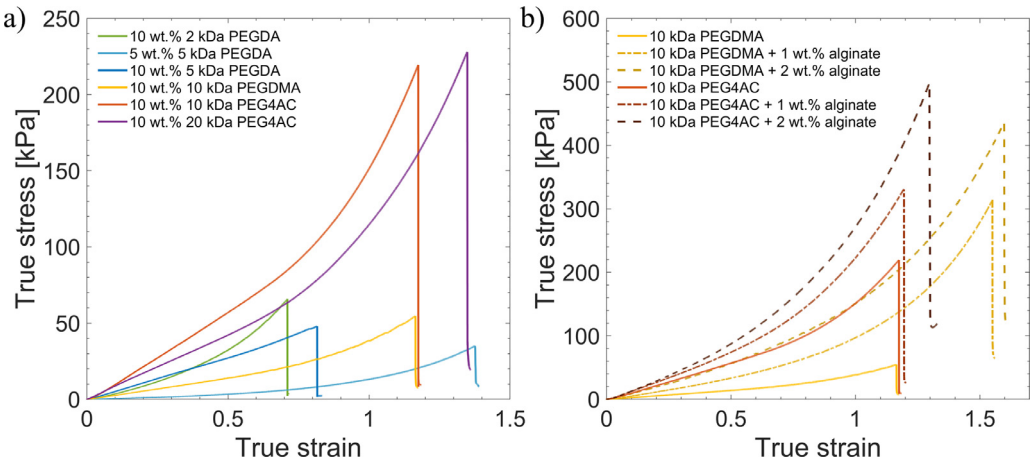


**Fig. 3.** (a) True stress-strain curves of PEG-based SN hydrogels and (b) true stress-strain curves of 10 wt.% 10 kDa PEG-based SN and DN hydrogels.

adding the second alginate network. Finally, Fig. 4 shows mean values of the modulus, strength, strain to failure, and toughness deduced for each group. Typically the averages were from 6 to 8 samples for each group, but for the more fragile groups the removal of damaged samples sometimes gave only 4 to 5 repeat tests for averaging.

For constant molecular weight (10 kDa) and mass fraction (10 wt.%), PEG SN hydrogels linked by 4-arm monomers demonstrated significantly ($p < 0.05$) higher modulus, compressive strength, and toughness compared to their linear monomer counterparts (Fig. 4). For constant monomer architecture and mass fraction, the mechanical properties of the SN hydrogels did not vary significantly with molecular weight and values of modulus, compressive strength, and toughness were quite similar for the various groups ($p > 0.05$). Finally, for the linear 5 kDa PEGDA monomers, experiments were conducted for both 5 wt.% and 10 wt.% SN hydrogels and while the modulus significantly ($p < 0.05$) decreased with decreasing mass fraction, the strength and toughness values were similar ($p > 0.05$) and the strain to failure of the 5 wt.% group was the highest of the linear monomer groups ($p < 0.05$).

Creating alginate reinforced DN hydrogels drastically increased all mechanical properties for all of the PEG-based hydrogels investigated (Fig. 4). Additionally, the influences of the PEG molecular weight and mass fraction became more pronounced for the DN hydrogels compared to the SN hydrogels. For DN gels with the same PEG monomer architecture, increasing monomer molecular weight resulted in a significant ($p < 0.05$) enhancement of all mechanical properties. However, when comparing the double network 4-arm and linear PEG results at 10 kDa MW, it is seen that the advantages of the 4-arm architecture are greatly diminished. While the 4-arm DN remained significantly ($p < 0.05$) stiffer, the modulus advantage was less, the strength and toughness were not significantly different ($p > 0.05$), and the strain to failure clearly became worse ($p < 0.05$) compared to the linear monomer architecture. Overall, when considering Fig. 4c, it is seen that the alginate reinforcement enhanced the strain to failure of the linear PEG networks more than

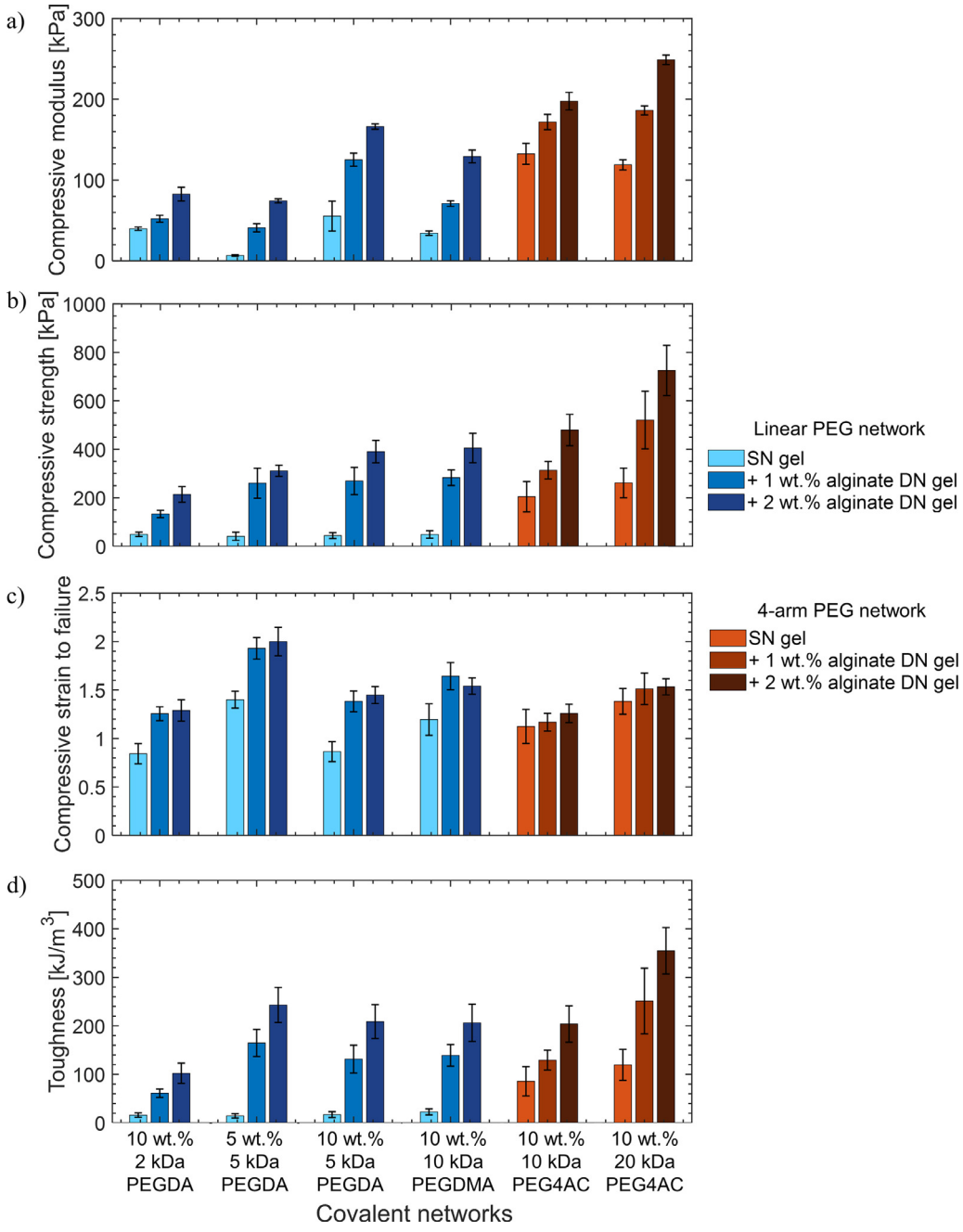


**Fig. 4.** Mechanical characterization results for the PEG-based SN and DN hydrogels: (a) compressive modulus, (b) compressive strength, (c) compressive strain to failure, and (d) toughness calculated as the area under the true stress-strain curves.

the 4-arm networks. Also of note are the results for the DN gels using the lower mass fraction, 5 wt.% linear 5 kDa PEGDA covalent network. While the SN gels were very weak with very low stiffness and toughness, the corresponding DN gels had by far the highest strains to failure (Fig. 4c) and the second highest toughness (Fig. 4d).

To understand if the addition of alginate significantly affected the strain rate sensitivity of the gels, 10 wt.% 10 kDa PEG4AC gels with 0 wt.% and 2 wt.% alginate were tested as representative groups using 0.01 mm/sec and 0.1 mm/sec loading rates until failure. As shown in Fig. 5, the modulus and stress at rupture for the single network PEG4AC hydrogel slightly decreased ($p < 0.05$) at the higher compression rate due to quicker breakage of covalent bonds under compression, while the compression responses of gels with 2 wt.% alginate under different rates were more similar. Overall, forming the alginate reinforced double network reduced the strain rate sensitivity. Indeed, results of the Kruskal-Wallis test showed no significant effect ($p > 0.05$) of compression rate on strength, strain to failure, or toughness of the DN gels and the effect on modulus was diminished ($p = 0.047$).

Finally, Fig. 6 shows hysteresis loops during cyclic loading of 10 wt.% 10 kDa PEG4AC based SN and DN gels. With higher amounts of alginate, more energy dissipation was observed. Compared to the SN gel (4.3 kJ/m$^3$), the DN gel with 1 wt.% alginate dissipated 4 times more energy (19.0 kJ/m$^3$) whereas the DN gel with 2 wt.% alginate exhibited significantly more hysteresis with 42.1 kJ/m$^3$ of

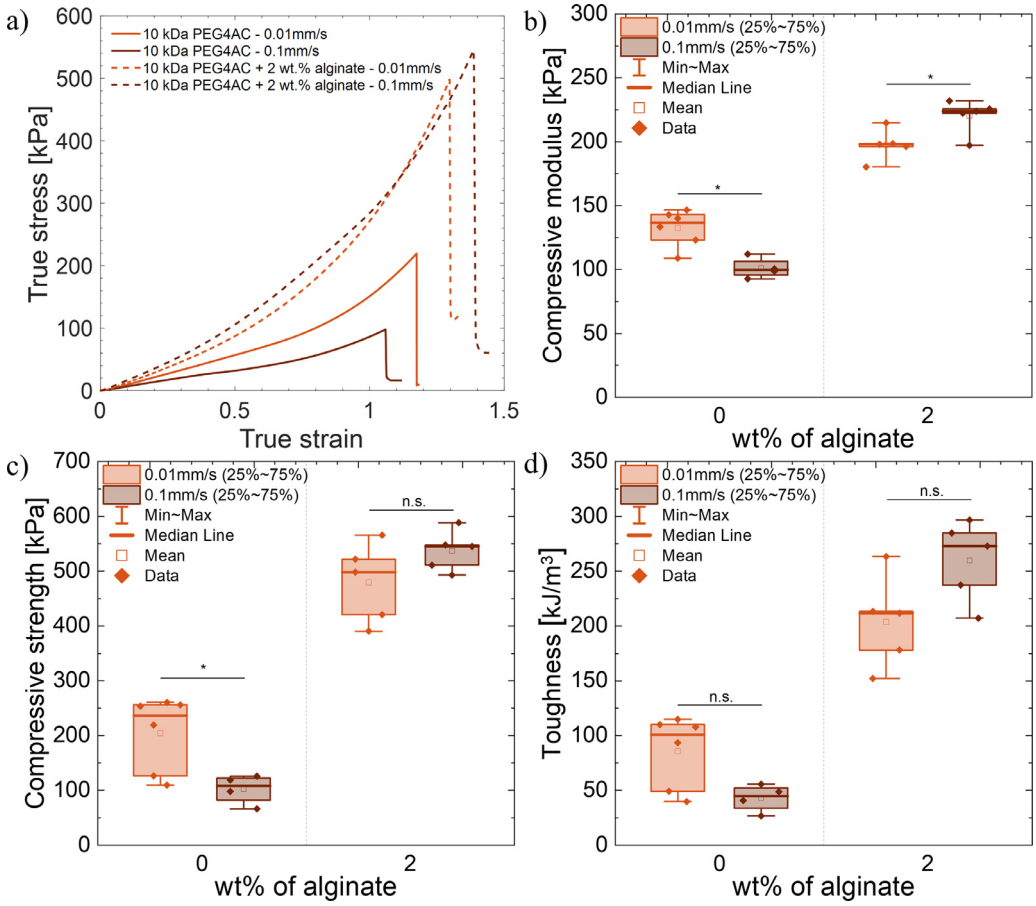


**Fig. 5.** (a) Typical true stress-strain curves for 10 wt.% 10 kDa PEG4AC SN hydrogel and DN hydrogel with 2 wt.% alginate. Comparison of (b) compressive modulus, (c) compressive strength and (d) toughness with two different compression rates showed that mechanical characteristics of PEG-alginate DN gels were not significantly rate-dependent. The label "n.s." indicates that the statistical tests did not reveal a significant difference and "*" represents a significant difference with $p<0.05$.

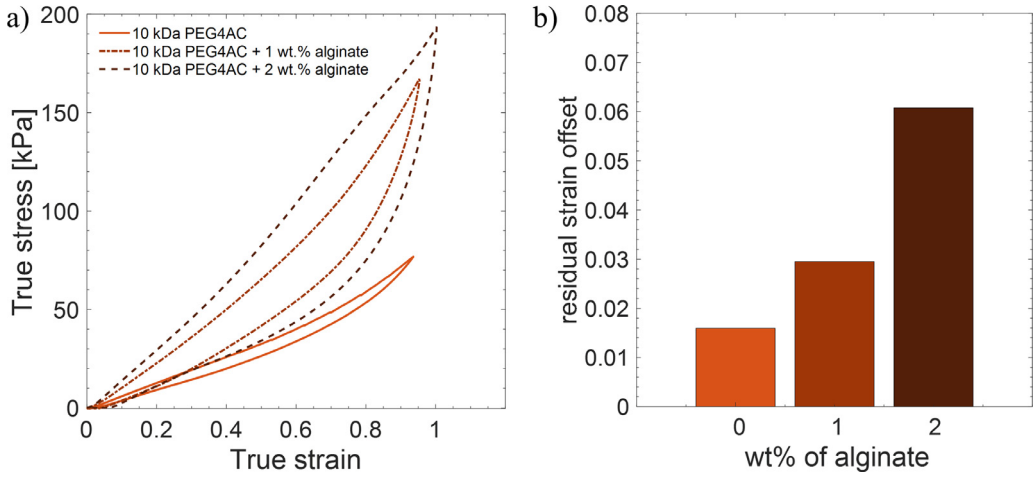


**Fig. 6.** (a) Stress-strain hysteresis and (b) residual strain offset of 10 wt.% 10 kDa PEG4AC-based SN and DN hydrogels.

energy dissipation. In addition, a decrease in sample height could be observed from DN gels after unloading, as shown by the residual strain offset seen in Fig. 6b upon unloading to zero force.

### 3.3. Cell adhesion on double network hydrogels

To understand how the increased mechanical properties (i.e., modulus) of double network hydrogels may influence the cell adhesion processes, we explored adhesion and spreading characteristics of ADSCs on SN and DN gels. We selected 10 kDa PEGDMA hydrogels, which show a monotonic increase in modulus from the SN (~24 kPa) to the 1 wt.% alginate DN (~71 kPa) and 2 wt.% alginate DN (~129 kPa). As can be seen from Fig. 7a, cells seeded on the DN gels (PEGDMA gels with 1 wt.% and 2 wt.% alginate) show significantly higher spreading at day 1 and day 7 compared to the SN gel.

ADSCs have previously been shown to differentiate in response to substrate stiffness through mechanotransduction involving the

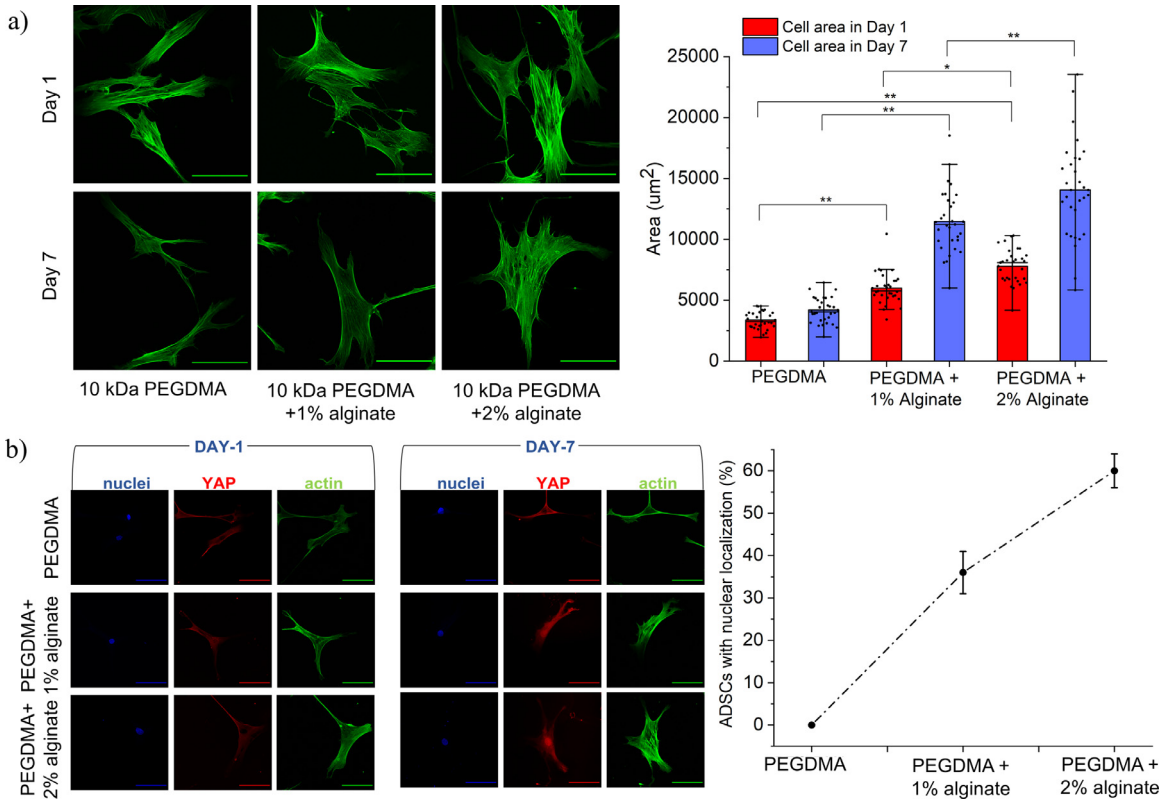


**Fig. 7.** (a) Representative fluorescence images of labeled filamentous actin in ADSCs cultured on different SN and DN PEG gels (scale bar=100 μm) and quantification of average cell area ($n$=30, number of cells). ("*" represents $p < 0.05$, "**" represents $p < 0.01$ in one-way ANOVA test.) (b) Representative images of ADSCs cultured on different SN and DN PEG gels after day 1 and day 7 (scale bar=100 μm) and YAP nuclear localization at day 7.

molecular mechanosensor Yes-associated protein (YAP), which is a transcriptional regulator whose shuttling between the cytoplasm and the nucleus is indicative of changing mechanical microenvironments [55,56]. Since our cells show significant changes in area when going from a SN to DN, we asked whether cell spreading is directing YAP activity in our ADSCs. Fig. 7b shows that in SN gels, YAP is primarily localized to the cytoplasm in both day 1 and day 7 experiments. However, adding alginate leads to a significant increase in YAP nuclear localization: 36% for cells adherent to the 1 wt.% alginate DN and 60% of cells adherent to the 2 wt.% alginate DN. Together, these experiments demonstrate that stiffening PEG-based hydrogels through double network formation with alginate leads to increases in both the cell spread area and the activation of mechanosensory elements.

## 4. Discussion

Previous studies have shown how the modulus of PEG based single network (SN) hydrogels can be increased by increasing the crosslink density in the hydrogel and/or decreasing the average molecule length between crosslinks (i.e., mesh size). This could be achieved by decreasing the molecular weight, increasing the mass concentration and/or switching to a multi-arm monomer architecture [35,39,40]. However, a comparison of strength and toughness has not generally been reported due to the weak and brittle nature of SN hydrogels. The advent of double network (DN) hydrogels opens up new potential applications such as medical adhesives, implant devices, or soft robotics where material strength and toughness will be of upmost importance. However, to date little is known about how to control the mechanical properties of hybrid DN hydrogels beyond changing the concentration of the physically bonded network [28,31]. Only one study has reported that an initially tougher SN will lead to a tougher DN [13] and questions remain about the detailed relationships between hydrogel structure, strength, deformability, and toughness. Therefore, the current study examines how to manipulate a wide range of mechanical properties by altering the structural features of the covalently crosslinked network through the monomer molecular weight and architecture. Furthermore, the results of this study provide some new understanding of how cells respond to the altered mechanical properties of hybrid DN hydrogels.

### 4.1. Effects of alginate concentration

The modulus and strength of all groups showed monotonic increases with increasing alginate from 0 to 2 wt.% (Fig. 4a, b). The increase in modulus can be explained by the additional alginate network increasing the overall network density, thus imparting additional stiffness. Similarly, the increase in strength arises from the alginate network shielding the covalent PEG network from experiencing some of the applied stress and thus delaying its fracture. Such results agree well with previous studies on alginate reinforced polyacrylamide networks [28,31]. If we examine this result in terms of the network parameters from the Arruda-Boyce model (Supplementary Material, Table S1), we see that for all groups the effective crosslink density increases significantly more than just a linear summation of the alginate network to the PEG network. We also observed that the extensibility of the chains was relatively unchanged by the addition of alginate for most of the hydrogels, i.e., the $N$ values were similar for most cases with and without alginate (Table S1). For the most brittle SN case (5 wt.% 5 kDa PEGDA) there was an apparent increase in the chain extensibility parame-

ter when adding alginate to form a DN; however, upon closer examination this was attributed to ill-defined fits for this parameter when the polymers fail well below their locking stretch.

In contrast, the benefits to deformability (i.e., strain to failure) saturated after adding only 1 wt.% alginate to the linear monomer PEG networks, and alginate provided little, if any, benefit to the strain to failure for the 4-arm monomer PEG networks (Fig. 1c). In the presence of alginate, the strain to failure of the DN gels appears to benefit from the looser covalent networks formed by the linear PEG monomers (Fig. 4) and at 10 kDa MW the strain to failure was clearly lower for the 4-arm compared to the linear monomer architecture. An even more extreme example of this can be seen in the fracture strains for the lower mass fraction (5 wt.%) linear 5 kDa PEGDA covalent network. For that case, the SN hydrogel was initially very weak with very low stiffness, yet it gave by far the highest strain to failure for the DN hydrogels (Fig. 4c). While this sample group was not originally planned for this study of MW and architecture, it is included here for comparison because of its interesting mechanical properties after alginate reinforcement. Indeed, this group revealed that there are two alternative paths to achieving relatively high toughness, energy absorbing DN hydrogels. One case is not surprising whereby the highest toughness was achieved by reinforcing the 20 kDa MW 4-arm covalent network that started with the highest combination of strength, deformability, and toughness as a single network, and then experienced an enhancement of all properties as a double network. This finding is similar to that reported previously [13]. However, interestingly the 5 wt.% 5 kDa MW linear covalent network gave the second highest toughness despite the abysmal initial strength of the SN gel. A previous study suggested toughness should monotonically increase with increasing PEG mass fraction from 10 to 20 wt.% [13]; however, the present result suggests good toughness can also be achieved by using very low mass fraction. In this case, the alginate network provides most of the strength, while the deformability of the loosely linked covalent PEG network combined with the energy dissipation ability of the alginate results in high toughness for the DN gel.

Some effect of strain rate is usually expected in hydrogel systems, and other studies on hybrid DN hydrogels [13,28,31,57] have found a stronger strain rate effect compared to the SN gels. However, Fig. 5 shows that the mechanical properties of the DN hydrogels are similarly or less sensitive to strain rate than their SN counterparts. This implies that the energy dissipation from $Ca^{2+}$ crosslinks breaking and reforming occurs quickly enough to be unaffected by strain rate in the quasi-static regime, making this toughening mechanism robust for many practical applications. However, it should be expected that for high-speed dynamic loading, some loss of toughness may occur when the $Ca^{2+}$ crosslinks cannot reform at the same rate as their breaking.

The hysteresis loops during cyclic loading shown in Fig. 6 demonstrate enhanced mechanical energy dissipation for the double networks that is caused by the breakage of ionic crosslinks in the reinforcement network. While the PEG4AC SN gel exhibited nearly full recovery along with low hysteresis, the DN gels displayed larger residual strain offsets after unloading and higher energy dissipation in the hysteresis curves with increasing mass fraction of alginate. This was attributed to the linked alginate chains unzipping at higher stress. While the alginate network has a large self-healing capacity, the crosslinking of the alginate upon unloading cannot follow the exact same path resulting in permanent deformation after unloading. Such results are similar to previous studies [13,28].

Finally, with regards to alginate concentration, a previous study on alginate reinforced polyacrylamide networks found that both the stretch and fracture energy of DNs increased initially with alginate additions and peaked between ~1 and 2 wt.% alginate before declining [28], while another study found a monotonic decrease in stretchability and fracture energy with increasing alginate from 2.3 wt.% to 6.4 wt.% [31]. Our findings that most mechanical properties increased from 1 to 2 wt.% alginate are consistent with those previous studies. Thus, 1 and 2 wt.% alginate were chosen for this study to examine the role of monomer MW and architecture in affecting the properties of DN hydrogels because it was expected to give near peak properties. Furthermore, adding more alginate made mixing of the monomers difficult prior to gelation due to the high liquid viscosity. The findings with regards to monomer MW and architecture affecting the DN mechanical properties will be discussed in the following sections.

### 4.2. Effects of molecular weight

For single network PEG based hydrogels, the networks formed by larger MW monomers have lower crosslinking density and longer PEG chains between crosslinks (smaller $n$ and larger $N$ in Table S1), and the looser network has a higher capacity for water uptake and swelling, as is seen in Fig. 2. A looser structure should generally have lower modulus [35,39]. However, at 10% mass fraction we observed little effect of MW on the SN hydrogel modulus (Fig. 4a), which has also been observed by others for SNs whereby the effect of modulus was weak or negligible at 10 wt.% but much stronger at 15 and 20 wt.% [35]. Similarly, while tensile fracture energy has been reported to increase with molecular weight for 20 wt.% SN hydrogels [13], in the present work the compressive fracture energy was relatively insensitive to MW for our 10 wt.% single network PEG based gels (Fig. 4d). Curiously, despite the lack of trend in modulus, we do see the expected increase in chain extensibility with increase in MW, though it is less than the 1:1 proportionality with MW that would be predicted directly from theory. We chose to keep the PEG monomer wt.% relatively low in this study to enable easy mixing of the double networks whereby adding alginate substantially increased the viscosity of the liquid prior to gelation.

Interestingly, the effects of PEG monomer molecular weight on the mechanical properties became significant for the DN gels. Fig. 4 shows that DN hydrogels formed using higher MW PEG-based covalent networks were stiffer, stronger, tougher, and more deformable than those produced using lower MW of the same monomer architecture. For modulus, this means that creating high modulus DN hydrogels requires the exact opposite approach compared to SN hydrogels, for which lower molecular weight is generally observed to give enhanced modulus. Furthermore, while the literature reports a tradeoff with toughness increasing, but modulus decreasing, when increasing the MW of single network PEG based gels [13,35,39], we found that all properties increase with increasing MW for the DN alginate reinforced hydrogels (Fig. 4).

The MW effect on modulus must be attributed to the relative ability of the alginate network to stiffen the hybrid DN hydrogel. Interpreted through the Arruda-Boyce model, this increasing MW effect manifests itself as an increase in effective network density (i.e., the higher $n$ values seen in Table S1) without sacrificing the previously mentioned increase in chain extensibility. A looser covalent network with larger mesh size (i.e., smaller $n$ and larger $N$ values in Table S1) provides more open volume for the alginate network to interpenetrate and form a tightly crosslinked ionically bonded network. Thus, using a higher MW PEG-based monomer enhances the contribution of the alginate to the overall DN modulus. However, the baseline modulus of the PEG based covalent network still makes a significant contribution to the overall stiffness, and thus the DNs formed from linear PEG monomers never match the modulus of DNs formed using 4-arm monomers.

Next, it can be interpreted that looser PEG networks with fewer crosslinks and longer PEG chains between the crosslinks should

be able to sustain larger amounts of elastic deformation. Indeed, the data in Fig. 4c show a clear trend of higher strain to failure for the SNs with higher molecular weight when all other variables are held constant. After adding a reinforcing network of alginate, the more deformable covalent network will have a better ability to bridge the micro-fractures in the alginate network and hold the whole structure together before complete failure of the double network occurs. Thus, a clear trend in higher strain to failure with higher MW is observed for the DN hydrogels produced with both linear and 4-arm PEG networks.

While compressive strength has rarely been reported for DN hydrogels, it will be increasingly important for more mechanically demanding applications such as medical implants, soft robotics, etc. Higher combinations of modulus and strain to failure will lead to higher overall strength, and since both properties increase with increasing MW, we see a similar trend in increasing strength with molecular weight. Toughness derives from the combination of strength and strain to failure. Again, with both properties increasing with MW, an increase in compression toughness with increasing MW is observed as well. A similar finding was reported in tension for alginate reinforced PEGDA gels with the PEG monomer molecular weight increasing from 6 kDa to 10 kDa [13].

### 4.3. Effects of monomer architecture (linear vs. 4-arm)

SN and DN hydrogels produced using both linear and 4-arm PEG monomers were compared at the same molecular weight of 10 kDa. For SN hydrogels, the 4-arm PEG network demonstrated significantly less swelling (Fig. 2) along with higher compressive modulus, strength, and toughness compared to the linear network (Fig. 4). This is expected since the 4-arm PEG monomers will form a tighter network with higher crosslinking density and smaller mesh size, as is shown schematically in Fig. 1 and has been reported by Browning et al. for single network hydrogels [39]. The swelling-adjusted model parameters in Table S1 (larger $n$ and smaller $N$) agree well with this concept. The network density of the 4-arm hydrogel network is a bit more than twice that of the linear network and its number of Kuhn segments between crosslinks is a bit more than half the linear network. This is expected since the linear network will inherently have more defects from looping and dangling chains [41,58,59]. Increased crosslinking is thus responsible for the higher stiffness and strength of the covalent 4-arm PEG network. Doubling the molecular weight of the 4-arm PEG to 20 kDa is expected to form a mesh size more similar to the 10 kDa linear PEG (Fig. 1); however, the 4-arm SN gel still performed stiffer, stronger, and tougher than the comparable linear SN gel. Here it is again interpreted that the 4-arm monomers form a covalent network structure with higher uniformity and fewer defects [18,41,60], as schematically illustrated in Fig. 1.

For the DN hydrogels, the addition of the alginate network diminished the mechanical property advantages of 4-arm architecture as shown in Fig. 4. At 10 kDa MW, the difference of the compressive modulus between the two DN gels with linear and 4-arm covalent network structures was less than for the SN gels, while the strength and toughness were not significantly different. The looser covalent network of the linear PEG with larger mesh size (smaller $n$ and larger $N$ in Table S1) appears to provide more ability for the alginate network to interpenetrate and form a tightly crosslinked ionically bonded network. Thus, the alginate contribution to increasing the overall DN mechanical properties becomes greater when using the linear PEG for the covalent network.

When considering all the various MWs in Fig. 4c, it is seen that there is a general trend of the alginate reinforcement increasing the strain to failure for the linear PEG networks more than for the 4-arm networks. At 10 kDa MW, the strain to failure was clearly lower for the 4-arm DNs compared to their linear counterparts despite being similar as single networks. Examining the model parameter fits (Table S1), the additional alginate network is primarily acting to delay catastrophic failure rather than altering the extensibility of the primary network chains themselves. Thus, the effect of switching from a 4-arm to a linear PEG network is thought to be similar to the effect of higher molecular weight, whereby the longer PEG chains in the linear PEG network can better bridge micro-fractures of the alginate network to delay overall fracture, thus resulting in a larger improvement of the strain to failure with alginate. There is, however, a secondary effect contributing to this strain to failure comparison: the double networks swell less with addition of alginate because of their increased overall crosslink density, which leads to chains that are less stretched at the start of the compression experiment. The linear polymer swelling is more sensitive to alginate content than the 4-arm and therefore its strain to failure benefits more from the alginate content. Thus, some tradeoffs are observed in modulus versus deformability; for a fixed molecular weight, the 4-arm PEG architecture does not appear to be the clear choice for enhanced mechanical properties of the hybrid double network hydrogels. However, when doubling the molecular weight of the 4-arm PEG to 20 kDa to make the mesh size more similar to the 10 kDa linear PEG (Fig. 1 and Table S1), the 4-arm DN gels provide better overall mechanical properties (Fig. 4).

### 4.4. Effects of double network on stem cell mechanotransduction

PEG-based hydrogels are common biomaterials for cell biology studies, and the degree of cell spreading has been directly linked to the stiffness of the underlying gel matrix. Adipose derived stem cells (ADSCs) are a promising cell source for regenerative medicine and represent a common ‘mechanosensitive’ model system to understand how cellular processes are dictated by substrate mechanical properties [61,62]. ADSCs show an increase in spread area when cultured on SN < DN (1 wt.% alginate) < DN (2 wt.% alginate) which corresponds to the increase in stiffness. This result is consistent with what is known about cell adhesion as it relates to stiffness. Increased rigidity leads to a faster assembly-disassembly of the adhesion contact points, which nucleates filamentous actin and increases cytoskeletal tension [63]. As culture times increase from 1 to 7 days, the cell area remains approximately the same for cells adherent to the SN gels. However, cells adherent to the DN gels show an increase in the average area over time; approximately 1.5× with a broader range of sizes. This result was somewhat surprising considering most previous work with mesenchymal cells demonstrate complete spreading within 1 day. Since the adhesion protein fibronectin was covalently conjugated to the alginate network, we speculate that the viscoelastic DN gels lead to partial non-linear mechanical response to cell-generated stress, which yields a broader range of cell shapes and sizes over time. This is consistent with reports of how non-covalent stabilized materials like alginate can show strain stiffening and softening, which will encourage mechanosensing over longer distances.

Further analysis of cell mechanochemical response indicates that ADSCs adherent to the SN gel have predominantly cytoplasmic localization of the stiffness-sensor Yes-associated protein (YAP) [55,56], with an increase in the number of cells expressing nuclear YAP with each increase in alginate content. This result is consistent with the role of YAP in conveying mechanical information to the nucleus of cells to regulate gene expression. Since ADSCs have been shown to increase nuclear YAP with increased stiffness, which also corresponds to the propensity for chondrogenesis and osteogenesis [64], DN gels may be a good candidate hydrogel system for promoting bone and cartilage differentiation.

## 5. Conclusions

Based on the study of the effects of PEG monomer molecular weight and architecture on mechanical properties of PEG single network (SN) and PEG-alginate double network (DN) hydrogels, the following conclusions can be drawn:

- While increasing the molecular weight of 10 wt.% SN PEG based hydrogels had little effect on the mechanical properties, in contrast, for the DN hydrogels all mechanical properties (modulus, strength, strain to failure, and toughness) increased significantly with increasing PEG molecular weight.
- The effect of MW was attributed to the looser network and larger mesh sizes of the higher MW covalent networks that (1) provide more open volume for the alginate network to interpenetrate and crosslink to stiffen and reinforce the hybrid structure and (2) provide more deformability of the covalent network to bridge the micro-fractures of the alginate network and hold the hybrid structure together before complete failure.
- At the same molecular weight of 10 kDa, 10 wt.% SN hydrogels using the 4-arm PEG based monomer outperformed the mechanical properties of their linear counterparts. However, for DN hydrogels this advantage was greatly diminished, with the moduli being closer together, the strength and toughness being indistinguishable, and the strain to failure clearly worse for the 4-arm monomer.
- The diminished effect of monomer architecture (linear vs. 4-arm) for the DN hydrogels was attributed to the looser covalent network of the linear network providing more ability for the alginate network to interpenetrate and crosslink to provide a larger contribution to the mechanical properties.
- Despite the dynamic nature of the ionic alginate network and its ability for bond breakage and reformation, the DN hydrogels showed less sensitivity to strain rate than their SN counterparts. Thus, it is concluded that the $Ca^{2+}$ crosslinks can break and reform quickly enough to be relatively unaffected by deformation rate changes in the quasi-static regime examined (0.01 –0.1 mm/s).
- The change in mechanical properties with addition of the alginate network leads to changes in adipose derived stem cell spreading and mechanosensing, which has the potential to be tuned to direct specific differentiation outcomes.
- Increasing mechanical properties through a second network influences the adhesion characteristics of adherent mesenchymal stromal cells, with increased spread area, nuclear localization of YAP.

Together, the findings of this study will be useful to enable the design of hydrogels with controllable mechanical and biological properties for engineering applications that require high strength and toughness alone (e.g., soft robotics) or in combination with favorable cell spreading and differentiation (e.g., medical implants, tissue engineering scaffolds, etc.).

## Declaration of Competing Interest

The authors declare that they have no known competing financial interests or personal relationships that could have appeared to influence the work reported in this paper.

## Acknowledgments

The authors greatly acknowledge the facilities provided by the Mark Wainwright Analytical Centre at the University of New South Wales. Financial support was provided by the Australian Research Council grants FT180100417 and DP210103654 and by the National Science Foundation under Grant No. CAREER-1653059.

## References

[1] P.C. Nicolson, J. Vogt, Soft contact lens polymers: an evolution, Biomaterials 22 (24) (2001) 3273–3283.
[2] T. Goda, K. Ishihara, Soft contact lens biomaterials from bioinspired phospholipid polymers, Expert Rev. Med. Devices 3 (2) (2006) 167–174.
[3] B. Balakrishnan, M. Mohanty, P. Umashankar, A. Jayakrishnan, Evaluation of an in situ forming hydrogel wound dressing based on oxidized alginate and gelatin, Biomaterials 26 (32) (2005) 6335–6342.
[4] E.A. Kamoun, E.-R.S. Kenawy, X. Chen, A review on polymeric hydrogel membranes for wound dressing applications: PVA-based hydrogel dressings, J. Adv. Res. 8 (3) (2017) 217–233.
[5] J. Li, D.J. Mooney, Designing hydrogels for controlled drug delivery, Nat. Rev. Mater. 1 (2016) 16071, doi:10.1038/natrevmats.2016.71.
[6] G.D. Nicodemus, S.J. Bryant, Cell encapsulation in biodegradable hydrogels for tissue engineering applications, Tissue Eng. Part B Rev. 14 (2) (2008) 149–165.
[7] K. Da Silva, P. Kumar, Y.E. Choonara, L.C. du Toit, V. Pillay, Three-dimensional printing of extracellular matrix (ECM)-mimicking scaffolds: a critical review of the current ECM materials, J. Biomed. Mater. Res. A 108 (12) (2020) 2324–2350.
[8] J.P. Gong, Y. Katsuyama, T. Kurokawa, Y. Osada, Double-network hydrogels with extremely high mechanical strength, Adv. Mater. 15 (14) (2003) 1155–1158, doi:10.1002/adma.200304907.
[9] A. Nakayama, A. Kakugo, J.P. Gong, Y. Osada, M. Takai, T. Erata, S. Kawano, High mechanical strength double-network hydrogel with bacterial cellulose, Adv. Funct. Mater. 14 (11) (2004) 1124–1128.
[10] L. Weng, A. Gouldstone, Y. Wu, W. Chen, Mechanically strong double network photocrosslinked hydrogels from N,N-dimethylacrylamide and glycidyl methacrylated hyaluronan, Biomaterials 29 (14) (2008) 2153–2163.
[11] C. Fan, L. Liao, C. Zhang, L. Liu, A tough double network hydrogel for cartilage tissue engineering, J. Mater. Chem. B 1 (34) (2013) 4251–4258.
[12] D. Myung, W. Koh, J. Ko, Y. Hu, M. Carrasco, J. Noolandi, C.N. Ta, C.W. Frank, Biomimetic strain hardening in interpenetrating polymer network hydrogels, Polymer 48 (18) (2007) 5376–5387.
[13] S. Hong, D. Sycks, H.F. Chan, S. Lin, G.P. Lopez, F. Guilak, K.W. Leong, X. Zhao, 3D printing of highly stretchable and tough hydrogels into complex, cellularized structures, Adv. Mater. 27 (27) (2015) 4035–4040.
[14] H. Xin, S.Z. Saricilar, H.R. Brown, P.G. Whitten, G.M. Spinks, Effect of first network topology on the toughness of double network hydrogels, Macromolecules 46 (16) (2013) 6613–6620.
[15] L. Tang, D. Zhang, L. Gong, Y. Zhang, S. Xie, B. Ren, Y. Liu, F. Yang, G. Zhou, Y. Chang, J. Tang, J. Zheng, Double-network physical cross-linking strategy to promote bulk mechanical and surface adhesive properties of hydrogels, Macromolecules 52 (24) (2019) 9512–9525.
[16] L. Jiang, C. Liu, K. Mayumi, K. Kato, H. Yokoyama, K. Ito, Highly stretchable and instantly recoverable slide-ring gels consisting of enzymatically synthesized polyrotaxane with low host coverage, Chem. Mater. 30 (15) (2018) 5013–5019.
[17] T. Murakami, B.V. Schmidt, H.R. Brown, C.J. Hawker, One-pot “click” fabrication of slide-ring gels, Macromolecules 48 (21) (2015) 7774–7781.
[18] T. Sakai, T. Matsunaga, Y. Yamamoto, C. Ito, R. Yoshida, S. Suzuki, N. Sasaki, M. Shibayama, U.I. Chung, Design and fabrication of a high-strength hydrogel with ideally homogeneous network structure from tetrahedron-like macromonomers, Macromolecules 41 (14) (2008) 5379–5384.
[19] P. Lin, S. Ma, X. Wang, F. Zhou, Molecularly engineered dual-crosslinked hydrogel with ultrahigh mechanical strength, toughness, and good self-recovery, Adv. Mater. 27 (12) (2015) 2054–2059.
[20] X. Xu, F.A. Jerca, V.V. Jerca, R. Hoogenboom, Covalent poly (2-isopropenyl-2-oxazoline) hydrogels with ultrahigh mechanical strength and toughness through secondary terpyridine metal-coordination crosslinks, Adv. Funct. Mater. 29 (48) (2019) 1904886.
[21] J.H. Lee, J. Park, J.-W. Park, H.-J. Ahn, J. Jaworski, J.H. Jung, Supramolecular gels with high strength by tuning of calix [4]arene-derived networks, Nat. Commun. 6 (2015) 6650, doi:10.1038/ncomms7650.
[22] X. Xu, F.A. Jerca, K. Van Hecke, V.V. Jerca, R. Hoogenboom, High compression strength single network hydrogels with pillar [5]arene junction points, Mater. Horiz. 7 (2) (2020) 566–573.
[23] Z. Wang, X. Zheng, T. Ouchi, T. Kouznetsova, H. Beech, S. Av-Ron, B. Bowser, S. Wang, J. Johnson, J. Kalow, Toughening hydrogels through force-triggered chemical reactions that lengthen polymer strands, Science 374 (6564) (2021) 193–196.
[24] J. Kim, G. Zhang, M. Shi, Z. Suo, Fracture, fatigue, and friction of polymers in which entanglements greatly outnumber cross-links, Science 374 (6564) (2021) 212–216, doi:10.1126/science.abg6320.
[25] N. Bosnjak, M.N. Silberstein, Pathways to tough yet soft materials, Science 374 (6564) (2021) 150–151.
[26] P.B. Jayathilaka, T.G. Molley, Y. Huang, M.S. Islam, M.R. Buche, M.N. Silberstein, J.J. Kruzic, K.A. Kilian, Force-mediated molecule release from double network hydrogels, Chem. Commun. 57 (68) (2021) 8484–8487.
[27] J.P. Gong, Why are double network hydrogels so tough? Soft Matter 6 (12) (2010) 2583–2590.
[28] J.-Y. Sun, X. Zhao, W.R.K. Illeperuma, O. Chaudhuri, K.H. Oh, D.J. Mooney, J.J. Vlassak, Z Suo, Highly stretchable and tough hydrogels, Nature 489 (7414) (2012) 133–136.
[29] K.Y. Lee, D.J. Mooney, Alginate: Properties and biomedical applications, Prog. Polym. Sci. 37 (1) (2012) 106–126.

[30] H. Xin, H.R. Brown, S. Naficy, G.M. Spinks, Mechanical recoverability and damage process of ionic-covalent PAAm-alginate hybrid hydrogels, J. Polym. Sci. B Polym. Phys. 54 (1) (2016) 53–63.
[31] J. Li, W.B.K. Illeperuma, Z. Suo, J.J. Vlassak, Hybrid hydrogels with extremely high stiffness and toughness, ACS Macro Lett. 3 (6) (2014) 520–523.
[32] C.H. Yang, M.X. Wang, H. Haider, J.H. Yang, J.-Y. Sun, Y.M. Chen, J. Zhou, Z. Suo, Strengthening alginate/polyacrylamide hydrogels using various multivalent cations, ACS Appl. Mater. Interfaces 5 (21) (2013) 10418–10422.
[33] J. Zhu, Bioactive modification of poly(ethylene glycol) hydrogels for tissue engineering, Biomaterials 31 (17) (2010) 4639–4656.
[34] X. Zhang, X. Guo, S. Yang, S. Tan, X. Li, H. Dai, X. Yu, X. Zhang, N. Weng, B. Jian, J. Xu, Double-network hydrogel with high mechanical strength prepared from two biocompatible polymers, J. Appl. Polym. Sci. 112 (5) (2009) 3063–3070.
[35] S. Lee, X. Tong, F. Yang, The effects of varying poly(ethylene glycol) hydrogel crosslinking density and the crosslinking mechanism on protein accumulation in three-dimensional hydrogels, Acta Biomater. 10 (10) (2014) 4167–4174.
[36] S. Lee, X. Tong, F. Yang, Effects of the poly(ethylene glycol) hydrogel crosslinking mechanism on protein release, Biomater. Sci. 4 (3) (2016) 405–411.
[37] J. Lee, M.N. Silberstein, A.A. Abdeen, S.Y. Kim, K.A. Kilian, Mechanochemical functionalization of disulfide linked hydrogels, Mater. Horiz. 3 (5) (2016) 447–451.
[38] M.J. Roberts, M.D. Bentley, J.M. Harris, Chemistry for peptide and protein PEGylation, Adv. Drug Deliv. Rev. 54 (4) (2002) 459–476.
[39] M.B. Browning, T. Wilems, M. Hahn, E. Cosgriff-Hernandez, Compositional control of poly(ethylene glycol) hydrogel modulus independent of mesh size, J. Biomed. Mater. Res. A 98A (2) (2011) 268–273.
[40] C. Wang, X. Tong, F. Yang, Bioengineered 3D brain tumor model to elucidate the effects of matrix stiffness on glioblastoma cell behavior using PEG-based hydrogels, Mol. Pharm. 11 (7) (2014) 2115–2125.
[41] C.C. Lin, K.S. Anseth, PEG hydrogels for the controlled release of biomolecules in regenerative medicine, Pharm. Res. 26 (3) (2009) 631–643.
[42] S. Lin-Gibson, S. Bencherif, J.A. Cooper, S.J. Wetzel, J.M. Antonucci, B.M. Vogel, F. Horkay, N.R. Washburn, Synthesis and characterization of PEG dimethacrylates and their hydrogels, Biomacromolecules 5 (4) (2004) 1280–1287, doi:10.1021/bm0498777.
[43] J.F. Lutz, Polymerization of oligo (ethylene glycol)(meth) acrylates: Toward new generations of smart biocompatible materials, J. Polym. Sci. Part A Polym. Chem. 46 (11) (2008) 3459–3470.
[44] H. Wang, S.M. Haeger, A.M. Kloxin, L.A. Leinwand, K.S. Anseth, Redirecting valvular myofibroblasts into dormant fibroblasts through light-mediated reduction in substrate modulus, PLoS One 7 (7) (2012) e39969.
[45] Y.S. Pek, A.C.A. Wan, J.Y. Ying, The effect of matrix stiffness on mesenchymal stem cell differentiation in a 3D thixotropic gel, Biomaterials 31 (3) (2010) 385–391.
[46] S.H. Parekh, K. Chatterjee, S. Lin-Gibson, N.M. Moore, M.T. Cicerone, M.F. Young, C.G. Simon, Modulus-driven differentiation of marrow stromal cells in 3D scaffolds that is independent of myosin-based cytoskeletal tension, Biomaterials 32 (9) (2011) 2256–2264.
[47] N. Huebsch, P.R. Arany, A.S. Mao, D. Shvartsman, O.A. Ali, S.A. Bencherif, J. Rivera-Feliciano, D.J. Mooney, Harnessing traction-mediated manipulation of the cell/matrix interface to control stem-cell fate, Nat. Mater. 9 (6) (2010) 518–526.
[48] H. Xin, H.R. Brown, S. Naficy, G.M. Spinks, Time-dependent mechanical properties of tough ionic-covalent hybrid hydrogels, Polymer 65 (2015) 253–261.
[49] W. Li, D. Wu, D. Hu, S. Zhu, C. Pan, Y. Jiao, L. Li, B. Luo, C. Zhou, L. Lu, Stress-relaxing double-network hydrogel for chondrogenic differentiation of stem cells, Mater. Sci. Eng. C 107 (2020) 110333.
[50] C. Yang, B. Han, C. Cao, D. Yang, X. Qu, X. Wang, An injectable double-network hydrogel for the co-culture of vascular endothelial cells and bone marrow mesenchymal stem cells for simultaneously enhancing vascularization and osteogenesis, J. Mater. Chem. B 6 (47) (2018) 7811–7821, doi:10.1039/C8TB02244E.
[51] M.S. Islam, T.G. Molley, J. Ireland, J.J. Kruzic, K.A. Kilian, Magnetic nanocomposite hydrogels for directing myofibroblast activity in adipose-derived stem cells, Adv. Biomed. Res. 1 (4) (2021) 2000072.
[52] M.C. Boyce, E.M. Arruda, Swelling and mechanical stretching of elastomeric materials, Math. Mech. Solids 6 (6) (2001) 641–659.
[53] J.A. Rowley, G. Madlambayan, D.J. Mooney, Alginate hydrogels as synthetic extracellular matrix materials, Biomaterials 20 (1) (1999) 45–53.
[54] E. Alsberg, K. Anderson, A. Albeiruti, R. Franceschi, D. Mooney, Cell-interactive alginate hydrogels for bone tissue engineering, J. Dent. Res. 80 (11) (2001) 2025–2029.
[55] C. Yang, M.W. Tibbitt, L. Basta, K.S. Anseth, Mechanical memory and dosing influence stem cell fate, Nat. Mater. 13 (6) (2014) 645–652.
[56] S.R. Caliari, S.L. Vega, M. Kwon, E.M. Soulas, J.A. Burdick, Dimensionality and spreading influence MSC YAP/TAZ signaling in hydrogel environments, Biomaterials 103 (2016) 314–323.
[57] X. Zhao, Multi-scale multi-mechanism design of tough hydrogels: building dissipation into stretchy networks, Soft Matter 10 (5) (2014) 672–687, doi:10.1039/C3SM52272E.
[58] Y. Gu, J. Zhao, J.A. Johnson, Polymer networks: from plastics and gels to porous frameworks, Angew. Chem. Int. Ed. 59 (13) (2020) 5022–5049.
[59] N.A. Peppas, Hydrogels in Medicine and Pharmacy: Fundamentals, CRC press, 2019, doi:10.1201/9780429285097.
[60] T.-S. Lin, R. Wang, J.A. Johnson, B.D. Olsen, Topological structure of networks formed from symmetric four-arm precursors, Macromolecules 51 (3) (2018) 1224–1231.
[61] J. Lee, A.A. Abdeen, X. Tang, T.A. Saif, K.A. Kilian, Matrix directed adipogenesis and neurogenesis of mesenchymal stem cells derived from adipose tissue and bone marrow, Acta Biomater. 42 (2016) 46–55.
[62] J. Lee, A.A. Abdeen, D. Zhang, K.A. Kilian, Directing stem cell fate on hydrogel substrates by controlling cell geometry, matrix mechanics and adhesion ligand composition, Biomaterials 34 (33) (2013) 8140–8148.
[63] P.A. Janmey, D.A. Fletcher, C.A. Reinhart-King, Stiffness sensing by cells, Physiol. Rev. 100 (2) (2020) 695–724.
[64] C.A. Shea, R.A. Rolfe, H. McNeill, P. Murphy, Localization of YAP activity in developing skeletal rudiments is responsive to mechanical stimulation, Dev. Dyn. 249 (4) (2020) 523–542.